# The shaping of planetary nebulae through interaction with the interstellar medium


Chris Wareing, Albert A. Zijlstra, Tim O'Brien

School of Physics and Astronomy, The University of Manchester


## Introduction

The accepted theory of planetary nebula (PN) formation is the interacting stellar winds model (ISW) (Kwok 1982, Balick 1987) where a fast wind (~1000 km s$^{-1}$) from the hot central star of a PN sweeps up the slow wind (~15 km s$^{-1}$) produced during the preceding asymptotic giant branch (AGB) phase. The swept-up dense shell is ionised by the energetic UV radiation of the central star, producing the familiar ring-like appearance of PNe.

Observations of PNe have shown several cases where the outer shell shows the only departure from symmetry and this has been proposed to be an effect of interaction with the interstellar medium (ISM). Recently, Villaver et al. (2003) (hereafter referred to as VGM) pointed out the PN—ISM interaction had only been studied by considering the relative movement when the nebular shell had already formed. They performed 2D hydrodynamic simulations following the full AGB and post-AGB (PN) phases and found that the interaction provides an adequate mechanism to explain the high rate of observed asymmetries in the external shells of PNe. Further, they concluded that stripping of mass downstream during the AGB phase provides a possible solution to the problem of missing mass in PN. Observational evidence for the effect of the ISM on AGB wind structures was found by Zijlstra (2002).

We have developed a 'triple-wind' model using an initial slow AGB wind, a subsequent fast post-AGB wind and adding a third wind reflecting the movement through the ISM into the ISW model. We are using a hydrodynamic scheme to investigate the effects of this triple-wind model on the formation of PNe and are comparing the results to recent observations of Galactic Bulge PNe.

The numerical scheme uses the second-order Godunov Scheme due to Falle (1991). The scheme is in 3D cartesian coordinates, fully parallel and includes the effect of radiative cooling. It is detailed in Wareing (2005). The simulations use a domain of $200^3$ cells and are performed in the frame of the central star (placed at cell coordinates 50,100,100). Mass-loss has been modelled according to the ISW model with a spherically symmetric constant mass-loss rate with constant velocity. Mass-loss is effected by artificially setting the density, momentum density and total energy density in a volume-weighted spherical region centred on the star, with a radius of 5¾ cells. The ISM is modelled with constant density. Movement through the ISM is parallel to the *x*-axis and material flows in at the (*x*=1) boundary with a positive *x*-velocity. All other boundaries are free-flow.

## Simulation parameters

An initial set of simulations varying only the relative velocity through the ISM were considered in Wareing (2005). We are now running a much larger set of simulations modeling the 500,000 yr evolution on the AGB. Selected simulations will be run on into the post-AGB phase. Typical estimates from the literature have been used for the constant wind parameter values. The constant AGB slow wind parameters are the velocity (15 km s$^{-1}$) and the temperature ($10^4$ K). We have used four values for the mass loss rate: $10^{-7}$, $5\times10^{-7}$, $10^{-6}$ & $5\times10^{-6}$ M$_\odot$ yr$^{-1}$. Selected simulations run on into the PN phase will use such parameters as a mass-loss rate of $5\times10^{-8}$ M$_\odot$ yr$^{-1}$, a velocity of 1000 km s$^{-1}$ and a temperature of $5\times10^4$ K. The switch between the AGB wind and the post-AGB wind will be instantaneous. In view of the still considerable uncertainties on the detailed properties and evolution of these winds, more detailed temporal variations have not been modeled. In reality, one may expect the AGB wind to show increasing mass-loss rates with time, whilst the post-AGB wind may increase in velocity over time. The gas pressure in all three winds is calculated assuming an ideal gas equation of state.

The ISM is assumed to be homogeneous with characteristics of a warm neutral medium (T = $8\times10^4$ K), the main constituent of the observed ISM. We have investigated three values of the ISM density – 2, 0.1 and 0.01 H cm$^{-3}$. Older stellar groups, to which PNe belong, are characterised by larger velocity dispersions and larger asymmetric drift velocities than younger stellar groups. Binney & Merrifield (1998) state asymmetric drift velocities are typically 20-30 km s$^{-1}$ and velocity dispersions are around 50 km s$^{-1}$ with individual velocities exceeding 100 km s$^{-1}$. Thick disk stars show higher asymmetric drift velocities and higher velocity dispersions. Halo objects do not participate in Galactic rotation and so show typical variations up to 200 km s$^{-1}$. With this velocity information in mind, we have chosen to investigate a range of stellar velocities in our simulations from 0 to 200 km s$^{-1}$ in steps of 25 km s$^{-1}$.

Due to time and computational constraints, we only considered three values of the AGB wind mass-loss rate for proper motions of above 100 km s$^{-1}$. This still led to a set of 93 simulations and an estimated computational processing time of over 40,000 single-CPU hours.

## Results and discussion

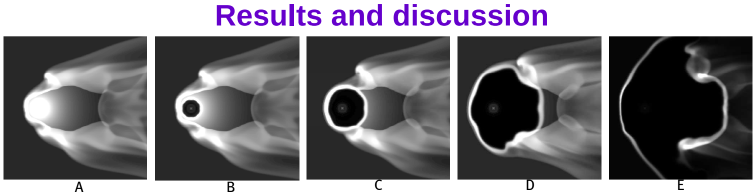


*Figure 1. Logarithmic density plots through the centre of the data cube showing the evolution of the PN-ISM interaction with the central star having a velocity of 100 km s$^{-1}$. The images are 1 pc on a side. Panel A is at the end of the AGB phase, B 1000 years into the PN phase, C 3000 yrs, D 6000 yrs and E 10,000 yrs.*

It is clear from our results that the interaction with the ISM strongly influences the environment in which the PN forms, as shown in Panel A of Figure 1. VGM points out that the problem in available models of PN-ISM interaction is that the interaction with the ISM had only been studied considering the relative movement when the PN had already formed. These models have clearly missed an important stage and the results of VGM in 2D are supported and extended by our 3D results.

Our results reveal a four stage evolution whereby in stage 1, the 'undisturbed' stage, the fast wind shell is initially unaffected by the movement through the ISM (see Figure 1, panel B). In stage 2, the 'brightening' stage, the PN brightens on the upstream side as the shell interacts with the AGB wind bow shock yet still appears circular on the sky (see Figure 1, panel C). In stage 3, the 'deviation' stage, the PN deviates from circular symmetry as the downstream part of the shell progresses down the tail (see Figure 1, panel D). At this stage the star appears to move upstream from the geometric centre of the nebula. Finally, in high speed cases (> 100 km s$^{-1}$) there is a fourth 'swept-downstream' stage where the fast wind has formed its own bow shock and the downstream portion of the shell has progressed beyond the tail of undisturbed AGB material (see Figure 1, panel E). Eventually the star will stop producing the fast wind and cease supporting any bow shocks. Ram pressure will drive the ancient nebula downstream beyond the central star and whilst a nebula may survive this, the central star will eventually appear to desert its nebula.

We find that PNe evolve quicker through these stages the faster they move through the ISM. This can be understood in terms of the AGB wind bubble being more confined at higher speeds and thus producing smaller nebula. The displacement in stage 3, originally thought to occur late in the evolution of PNe, can therefore occur early on when the central star has a high proper motion. Thus, displacement is NOT an indicator of an old PN. PNe with large AGB wind bow shocks can re-brighten late in life when the PN eventually enters stage 2 and interacts with AGB wind bow shock. Much of the mass lost during the AGB phase is stripped downstream, from 65% at a proper motion of 25 km s$^{-1}$ to 90% at 175 km s$^{-1}$. This effect provides a possible explanation of the missing mass problem observed in PNe.

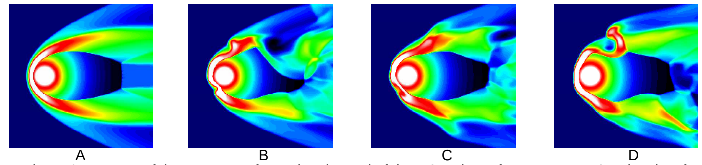


*Figure 2. A range of the structures formed at the end of the AGB phase for a constant ISM density of 2 H cm$^{-3}$ and a constant proper motion of 75 km s$^{-1}$. The mass-loss rate increases from left to right as does the size of the domain. Panel A: $\dot{M} = 10^{-7}$ M$_\odot$ yr$^{-1}$, 0.25 pc on a side; panel B: $\dot{M} = 5\times10^{-7}$ M$_\odot$ yr$^{-1}$, 0.6 pc on a side; panel C: $\dot{M} = 10^{-6}$ M$_\odot$ yr$^{-1}$, 0.8 pc on a side; panel D: $\dot{M} = 5\times10^{-6}$ M$_\odot$ yr$^{-1}$, 1.75 pc on a side.*

Given the interaction during the AGB phase, PNe observed to be interacting with the ISM are not necessarily ancient, nor require high proper motions or magnetic fields. Our simulations have shown that interaction can become apparent at a young age via several methods and that central stars with an average proper motion can show evidence of interaction in their nebulae, as commonly observed, and be displaced from the geometric centre.

In these simulations we see instabilities forming in the AGB wind bow shock at speeds of 50 km s$^{-1}$ and above (see Figure 2). These are thought to be formed by vortex shedding from the head of the bow shock. When a fluid passes by an object, or in this case the ISM flowing past the AGB wind bubble of the central star, the shear layer near the object, in this case the forward shock, has a high velocity gradient, making it inherently unstable. Further downstream, the forward shock and regions behind it break down into well defined vortices which then flow downstream, similar to terrestrial vortex streets. These vortices can alter and possibly enhance mixing of stellar material back into the ISM. This is the first discussion of these instabilities in this area of astrophysics.

These conclusions are in agreement with the conclusions reached by VGM using similar models. We have extended the study of the PN-ISM interaction including the AGB phase to three dimensions investigating higher proper motions, varying mass-loss rates on the AGB and varying ISM density.

## An application of the model: Sh 2-188

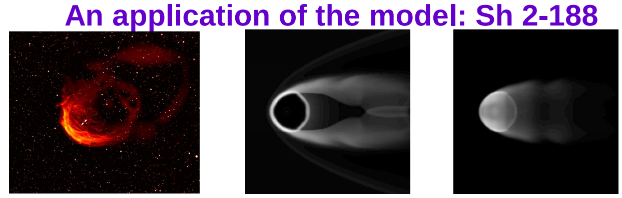

*Figure 3. On the left is an artificial combination of two three-colour images of the PN Sh 2-188, one scaled to show the bright filamentary structure, the other the faint structure. Hα is coded in red and yellow. The central star of the PN is marked between white diagonals. In the middle is a density slice through the simulation 20,000 years into the PN phase and on the right is the naïve simulated emission.*

Sh 2-188 is a galactic plane PN shown in the left panel of Figure 4. Until recently it was thought to consist only of the bright south-eastern filamentary arc, but new IPHAS observations (Drew et al. 2005) have revealed faint structure behind the nebula, closing the arc with a tail stretching behind the nebula. It has been postulated to be interacting with the ISM and we undertook simulations to model the object (Wareing et al. 2006). We found the object could be simulated in terms of a star moving at 125 ± 25 km s$^{-1}$ through the ISM (see the middle and right-hand panels of Figure 3). The tail structure formed during the AGB and the expanding PN shell is now interacting with the AGB wind bow shock upstream – the PN is in the 'brightening' stage. With this model in mind, we carried out a proper motion study of the central star (marked in Figure 3) and found a motion of 30 ± 10 milliarcseconds yr$^{-1}$ in the direction of the bright arc, as implied by the model. From this, we derived a distance estimate of 850 pc ± 500 pc and an age of 22,500 yrs ± 2,500 yrs, in agreement with spectroscopic estimates of the distance and age of the PN. Expansion velocities measured from the bright filaments are in agreement with our simulation. Further, our predicted local ISM density of 0.01 H cm$^{-3}$ is in agreement with the local electron density, assuming 1 H per electron, measured from pulsar dispersion measures. Sh 2-188 is thus one of the largest PN known, with a diameter of 2.8 pc: a size already set during the AGB phase. We estimate 2/3 of the mass introduced into the stellar region has been swept downstream.

## Future comparisons: Galactic bulge PNe

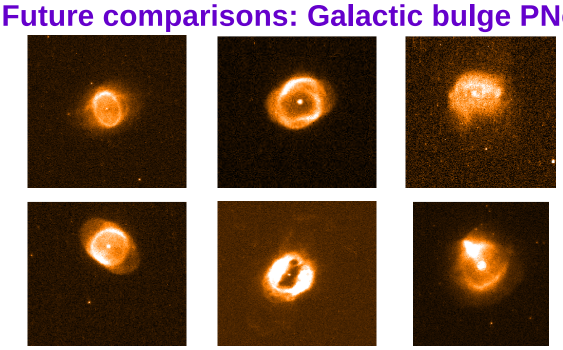

*Figure 4. A selection of Galactic Bulge PNe from a HST survey carried out by Zijlstra et al.*

In the future we intend to compare our simulations to recent observations of PNe in the Galactic bulge, many of which appear to be interacting with the ISM in some way (see Figure 4). The bulge is characterised by high velocity dispersions: on average both the line of sight dispersion and average proper motion are around 80 km s$^{-1}$. Thus, many of the PN in the Galactic bulge should be interacting with the ISM.

## References


Balick B., 1987, AJ, **94**, 671

Binney J. & Merrifield M., 1998, 'Galactic Astronomy'

Drew J.E. et al., 2005, MNRAS, **317**, 460

Falle S.A.E.G. 1991, MNRAS, **250**, 581

Kwok S. 1982, AJ, **258**, 280

Villaver E. et al., 2003, ApJL, **585**, L49; VGM

Wareing C.J., 2005, PhD Thesis, Univ. of Manchester

Wareing C.J. et al., 2006, MNRAS, **366**, 387

Zijlstra A.A. & Weinberger R, 2002, ApJ, **572**, 1006